



Cite this: *Mater. Horiz.*, 2024, 11, 2077

Received 15th October 2023,
Accepted 8th February 2024

DOI: 10.1039/d3mh01698f

rsc.li/materials-horizons

Fluorescent covalent organic frameworks – promising bioimaging materials

Chimatahalli Santhakumar Karthik,^{abc} Tina Skorjanc ^d and Dinesh Shetty ^{*,bc}

Fluorescent covalent organic frameworks (COFs) have emerged as promising candidates for imaging living cells due to their unique properties and adjustable fluorescence. In this mini-review, we provide an overview of recent advancements in fluorescent COFs for bioimaging applications. We discuss the strategies used to design COFs with desirable properties such as high photostability, excellent biocompatibility, and pH sensitivity. Additionally, we explore the various ways in which fluorescent COFs are utilized in bioimaging, including cellular imaging, targeting specific organelles, and tracking biomolecules. We delve into their applications in sensing intracellular pH, reactive oxygen species (ROS), and specific biomarkers. Furthermore, we examine how functionalization techniques enhance the targeting and imaging capabilities of fluorescent COFs. Finally, we discuss the challenges and prospects in the field of fluorescent COFs for bioimaging in living cells, urging further research in this exciting area.

Wider impact

The current review discusses a relatively new field of fluorescent covalent organic frameworks (COFs) that have been implemented as bioimaging tools. The design of these materials is highlighted, including strategies used to enhance the fluorescence properties of COFs, such as liquid phase exfoliation, incorporation of AIEgens, and rational pKa engineering. On account of their chemical stability, biocompatibility, photostability, and tunable structures, COFs not only rival existing cell imaging probes but can also be used as theranostic platforms to simultaneously deliver therapeutic substances while also serving as imaging tools. We believe that future developments in this field will involve bioimaging of more complex phenomena, for instance, simultaneous imaging of multiple targets, as well as more *in vivo* imaging that is currently limited to the zebrafish and mouse models. In terms of structural COF developments, more probes active in the NIR region will likely be designed in order to reach these two goals. This review presents the various design strategies used in the preparation of the current COF bioimaging probes, so it will greatly aid in the preparation of future COFs for the imaging of more complex cellular processes and disease states.

Introduction

Bioimaging technologies play a crucial role in ongoing research endeavors, aiding in the identification of biomarkers, studying disease progression, and evaluating the effectiveness of innovative therapeutic interventions. Researchers and clinicians leverage these cutting-edge imaging techniques not only for diagnostic purposes but also for advancing our understanding of complex diseases at the molecular and cellular levels.¹ In the ever-evolving landscape of modern healthcare, the synergy

between different imaging technologies represents a significant advancement, particularly in the realm of bioimaging research and development. The diagnosis and treatment of severe diseases, such as cancer and Parkinson's, present formidable challenges in contemporary medicine due to their significant mortality risks.^{1–4}

Early detection of malignancies is crucial for improving patient survival rates. In contemporary clinical settings, a diverse array of imaging techniques is employed, including magnetic resonance imaging (MRI), computed tomography (CT), photoacoustic (PA) imaging, positron emission tomography (PET), photothermal (PT) imaging, single-photon emission computed tomography (SPECT), and fluorescence (FL) imaging.^{5,6} These modalities are often combined synergistically, incorporating two or three techniques to generate comprehensive images with sufficient resolution and details for informed medical decision-making. This multi-modal approach enables clinicians to gather diverse information, leading to more

^a Department of Chemistry, SJCE, JSS Science and Technology University, Karnataka, 570 006, Mysore, India

^b Department of Chemistry, Khalifa University of Science and Technology, 127788, Abu Dhabi, United Arab Emirates. E-mail: dinesh.shetty@ku.ac.ae

^c Center for Catalysis and Separations (CeCaS), Khalifa University of Science and Technology, 127788, Abu Dhabi, United Arab Emirates

^d The Materials Research Laboratory, University of Nova Gorica, Vipavska 11c, 5270, Ajdovscina, Slovenia



accurate diagnoses and the development of tailored treatment plans.^{7,8}

In the multifaceted landscape of modern oncology, the intertwined fields of tumor imaging and therapy stand at the forefront, representing pivotal pillars in the fight against cancer. Tumor imaging serves as the vanguard, providing clinicians with the means to visualize and characterize tumors with unprecedented precision. From the early detection of minute lesions to the comprehensive staging of advanced malignancies, imaging modalities such as MRI, CT scans, PET scans, and ultrasound have revolutionized our diagnostic capabilities.⁶⁻⁸ These imaging techniques not only facilitate the localization and characterization of tumors but also play a pivotal role in guiding therapeutic interventions, monitoring treatment responses, and assessing disease progression. The synergy between tumor imaging and therapy is undeniable, with imaging modalities often serving as the



Chimatahalli Santhakumar Karthik

Chimatahalli Santhakumar Karthik received his PhD degree (2018) in Chemistry from the Visvesvaraya Technological University (VTU), India. He currently holds the position of Assistant Professor in the Department of Chemistry, JSS Science and Technology University. In 2023, he was a visiting scientist in Prof. Shetty's research group at Khalifa University, UAE. His area of expertise encompasses drug design, organic chemistry, polymeric materials and computational chemistry.



Tina Skorjanc

Tina Skorjanc was born in Maribor, Slovenia in 1992. She obtained her PhD from New York University in 2020, working on porous polymers and covalent organic frameworks (COFs) for water purification and drug delivery applications. In 2021, she was awarded a Marie Skłodowska Curie Widening Fellowship to apply these classes of materials to the study of biosensors at the university of Nova Gorica, Slovenia.

In 2023, she relocated to the Furukawa-Inose group at Kyoto

University, where she is developing hybrid materials for single cell endoscopy under the auspices of the Japanese Society for Promotion of Science (JSPS).

linchpin for personalized treatment planning, enabling clinicians to tailor therapeutic regimens to individual patients based on the specific characteristics and dynamics of their tumors.^{4,5,8}

FL bioimaging is a powerful technique that utilizes fluorescent molecules or nanomaterials to observe biological processes or structures in living cells or tissues. It provides detailed information about biomolecules, including proteins, nucleic acids, metal ions, reactive oxygen species (ROS), and neurotransmitters.⁹⁻¹¹ The advantages of fluorescence bioimaging over other imaging techniques include high sensitivity, high resolution, fast feedback, non-invasiveness, and harmless radiation.¹² It enables monitoring of cellular functions like enzyme activity, membrane potential, pH, and calcium signaling, and plays a crucial role in disease diagnosis, tracking treatment outcomes, and assisting surgical procedures.¹³⁻¹⁵ The field of fluorescence bioimaging, however, also faces challenges such as tissue absorption and scattering, autofluorescence interference, a low signal-to-noise (SNR) ratio, and limited tissue penetration depth.¹⁶ To address these challenges, researchers have been developing novel fluorescent probes and nanomaterials with improved optical properties, biocompatibility, stability, targeting ability, and activatability.^{16,17} In particular, fluorescence bioimaging in the second near-infrared window (NIR-II, 1000–1700 nm) has shown promise for deep tissue imaging with high contrast and low background.^{12,16} Achieving fluorescence bioimaging in the NIR-II window requires suitable fluorophores with emission wavelengths in this region. However, the development of efficient synthetic methods and design principles for NIR-II fluorophores remains challenging. Moreover, NIR-II fluorophores need to meet specific criteria for biomedical applications, including high fluorescence quantum yield, good photostability, biocompatibility, water solubility, easy functionalization, and low toxicity.^{16,17} To date, various types of NIR-II fluorophores have been developed based on different materials



Dinesh Shetty

Dr Dinesh Shetty holds a PhD degree (2011) in chemistry from Seoul National University, Korea. He pursued postdoctoral research at Emory University, USA, POSTECH, Korea, and NYUAD, UAE before starting his independent career at Khalifa University, UAE in 2019. He is the recipient of the Young Investigator Award from both the Korean Society of Nuclear Medicine and the Korean Cancer Research Foundation. His research interest is focused on developing multifunctional polymers and frameworks for various applications, including energy, water purification, and biomedical science. In his free time, he writes poems and newspaper column articles and podcasts his thoughts.



and structures, including inorganic nanoparticles, organic macromolecules, small molecules, and hybrid systems.^{12,16,17}

Fluorescent dyes specifically designed for bioimaging applications typically have a flat and symmetrical molecular structure, which helps them absorb NIR light more effectively.¹⁸ This molecular design enhances energy transfer processes and leads to higher fluorescence quantum yields in the NIR range.¹⁹ Through careful optimization of the dye's structure and conjugation system, researchers have successfully developed a wide range of NIR fluorophores with improved optical properties for bioimaging in the NIR-II window.^{20,21} These dyes offer several advantages, including increased tissue penetration depth, reduced scattering, and absorption in biological samples, and minimized background signal interference, thereby enabling highly sensitive and high-contrast deep-tissue imaging.^{21,22} Moreover, fluorescence bioimaging extensively utilizes fluorescent nanomaterials like quantum dots, carbon dots, gold nanoclusters, and upconversion nanoparticles.^{23–27} These materials are preferred due to their remarkable brightness, ability to withstand repeated exposure to light, customizable emission properties, and multiple functionalities. They offer valuable insights into the structure and function of biological systems that are not attainable through alternative techniques. These materials allow us to uncover the molecular makeup, precise positioning, interactions, and movement of biomolecules within living cells or tissues.^{23,26,27}

The effectiveness of FL imaging currently relies on the photophysical properties of fluorescent dyes (FDs), including their excellent photostability and large Stokes shift, as well as their concentration at the target site.^{28,29} Various organic FDs such as porphyrin, Nile red,³⁰ BODIPY,³¹ fluorescein-5-isothiocyanate,³² and rhodamine³³ have been developed to achieve the desired FL signal output and high SNR. However, a major challenge lies in the poor accumulation of FDs in tumors, resulting in a low SNR during the diagnostic process. To overcome this issue, novel nanodelivery systems have been designed to incorporate FDs into nanocarriers like inorganic nanoparticles, polymers, and liposomes.^{31,34–36} For example, researchers have developed polymer-based nanoparticles that encapsulate NIR FDs for FL imaging-guided synergistic cancer therapy.³⁷ Another study utilized Au nanoclusters as efficient nanocarriers to load FD molecules for tumor FL imaging and photodynamic therapy. However, the loading efficiency of these nanocarriers is relatively low (typically less than 10.0 wt%), leading to a low concentration of FD accumulation at the tumor site. Consequently, higher concentrations of agents are required to obtain FL images with a high SNR, which may result in side effects and restrict the practical applications of these delivery systems.^{34,35} To address this limitation, strategies have been proposed to enhance the loading capacity of FDs. By improving the loading capacity, it becomes possible to achieve higher concentrations of FDs at the tumor site, thereby enhancing the SNR of FL imaging.³⁸ These advancements in FD delivery systems hold promise for enhancing the efficacy and accuracy of FL imaging in various biomedical applications.

Conventional fluorescent materials used in bioimaging, such as organic dyes, fluorescent proteins, metal complexes,

and semiconductor nanocrystals, have their advantages and disadvantages. Their limitations include (i) photobleaching, (ii) phototoxicity, (iii) spectral overlap, (iv) limited emission wavelengths, (v) size and cellular uptake, (vi) toxicity and biocompatibility, (vii) genetic manipulation requirements, and (viii) limited sensitivity and resolution.^{26,28,39–44}

To overcome these limitations, alternative fluorescent materials for specific bioimaging experiments are required. These materials should have unique properties and advantages for bioimaging applications, such as improved brightness, photostability, multiplexing capabilities, deep tissue imaging, and reduced interference from background signals.

Overview of biomedical applications of COFs

In recent years, the remarkable properties of covalent organic frameworks (COFs), characterized by π -conjugation, low density, robust stability in diverse environments, adjustable porosity, large surface area, and biocompatibility, have propelled them to the forefront of biomedical applications.^{45,46} COFs, with their adjustable pore sizes and surface functionalization, stand as highly favorable platforms in drug delivery, ushering in a paradigm shift in therapeutic strategies. This adaptability allows for the controlled release of therapeutic agents, ensuring precise targeting of specific tissues or cells. The result is not only heightened therapeutic efficacy but also the minimization of off-target effects and systemic toxicity.^{47,48} The organic skeletons of COFs with lightweight elements make them more suitable candidates than metal–organic frameworks (MOFs) for drug delivery. The responsive nature of COFs to biological stimuli, such as pH, enzymes, or ROS, adds a layer of sophistication to drug delivery systems. This capability is harnessed to trigger the precise release of therapeutic compounds directly at the target site, promising more effective and targeted treatment approaches. Beyond drug delivery, COFs have emerged as promising candidates in cancer therapy, particularly in photodynamic therapy (PDT) and photothermal therapy (PTT).^{49–52} By incorporating photosensitizers or photothermal agents into COF structures, they can be activated with specific wavelengths of light. This localized activation induces ROS for PDT or generates heat for PTT, resulting in targeted cancer cell death while sparing surrounding healthy tissues.^{4,48,53} The versatility of COFs extends to biosensing applications, where the integration of recognition elements allows for the selective capture and detection of biomolecules or ions. This capability holds great promise for early disease detection, therapeutic response monitoring, and environmental sensing.^{54,55}

A comparison with MOFs

Currently, researchers have extensively explored various substances, including graphene, black phosphorus, hexagonal boron nitrides, transition metal dichalcogenides, MXenes, MOFs, metal and metal oxide nanosheets, and graphitic carbon



nitrides for applications in the field of biomedicine. Despite their diverse applications, most of these materials, excluding graphene and g-C₃N₄, pose challenges due to their intrinsic atomic thickness, resulting in issues related to poor mechanical flexibility and insufficient biocompatibility at the material-biological interface. Unlike graphene and g-C₃N₄, most organic materials suffer from low stability and limited loading capacities *in vivo*. On the other hand, inorganic substances often exhibit poor degradability and undesirable toxicity.^{56–62}

MOFs have attracted attention because of their large pore sizes, high surface areas, and good biodegradability. However, they have raised concerns about their chemical stability and toxicity in biomedical applications. MOFs are often susceptible to chemical degradation, especially in the presence of biological fluids. The instability of metal-organic coordination bonds under physiological conditions can limit their long-term performance in biological environments. MOFs contain metal ions, and the potential toxicity of these metals is a significant concern in biomedical applications. The release of metal ions from the framework could lead to undesirable toxic effects, making them less suitable for certain medical applications.^{58,63} In contrast to many reported MOFs, the robust chemical linkages inherent in COFs provide the necessary material stability in aqueous environments. Unlike several MOFs, the enduring chemical bonds of COFs ensure resilience and durability when exposed to water, a critical factor for biomedical applications. COFs offer the potential to achieve multimodal functionality through either pre-synthetic or post-synthetic integration of biologically important chromophores. This versatility in functionalization provides COFs with a distinct advantage over certain MOFs, enabling the incorporation of various functionalities within a single material and expanding the range of applications in biomedicine. The scope of integrating suitable molecular building blocks in COFs allows for the pre-designed functionality of the material. This characteristic grants the ability to tailor COFs for specific biomedical applications, leading to the facile formation of diverse nanoscale structures with controlled sizes and shapes.^{63,64} While MOFs are versatile, they might encounter limitations in precisely pre-designing functionality due to their reliance on metal nodes and organic linkers, which may not always offer the same level of predictability as COFs. The current review lies in its focused exploration of fluorescent COFs specifically for bioimaging applications. It thoroughly examines the fluorescence mechanism, structural considerations, and challenges associated with large-scale production and biological interactions. The forward-looking section offers a roadmap for future research in addressing the challenges and maximizing the potential of fluorescent COFs in bioimaging.

Fluorescent covalent organic frameworks (COFs)

Fluorescent COFs have garnered attention as a promising option for bioimaging. COFs are crystalline porous materials made up of organic building blocks linked by covalent bonds.

They possess distinctive characteristics such as a large surface area, adjustable pore sizes, and structural flexibility, which can be beneficial for bioimaging purposes.^{39,40,66}

Structural symphony of COFs in bioimaging

The natural fluorescence inherent in COFs positions them as valuable contrast agents in bioimaging, emitting light upon excitation. Their designable and modular nature allows for meticulous control over their structure, particularly in tuning the π -conjugated system. This tunability facilitates the adjustment of emission wavelengths, aligning them with desired imaging conditions. This adaptability minimizes background interference, heightening imaging specificity. The porous characteristics of COFs, coupled with a substantial surface area, create sites for integrating imaging agents, contrast agents, or other functional molecules. This porous nature enhances COFs' versatility in bioimaging, fostering the creation of multi-functional imaging platforms. COFs boast ease of functionalization achieved by incorporating diverse building blocks during synthesis or through post-synthetic modifications.^{39,40} This adaptability enables the introduction of specific functional groups or moieties, amplifying imaging capabilities, enabling targeted imaging, or responding to environmental stimuli. Moreover, certain COFs can be tailored to be responsive to environmental factors like pH variations or the presence of particular biomolecules. This responsiveness proves beneficial for targeted imaging or triggering specific imaging responses under defined conditions. The multifaceted attributes of COFs, ranging from their inherent fluorescence to tunable structures, porous nature, and functionalizability, underscore their significance in bioimaging, allowing for sophisticated and tailored imaging approaches.⁶⁵ However, it is important to acknowledge that the practical application of fluorescent COFs in this field is still relatively new. Further research is necessary to fully explore their potential. There are challenges to address, including optimizing their fluorescence properties, reducing their particle size, enhancing biocompatibility, and evaluating their performance in complex biological systems. Nevertheless, fluorescent COFs offer an exciting avenue for advancing bioimaging techniques, particularly on account of their unique advantages in stability, adjustable properties, and the possibility of functionalization. However, it is important to note that the direct use of fluorescent COFs for *in vivo* imaging is still limited, primarily due to the aggregation-caused quenching (ACQ) effect caused by the strong conjugation of FDs in COFs. Consequently, there is a need for further research and exploration of the potential applications of COFs in *in vivo* imaging.

Fluorescence mechanism in COFs

The fluorescence mechanism in COFs primarily originates from the presence of fluorophores within their framework.⁶⁶ These fluorophores typically consist of organic chromophores or aromatic moieties with conjugated π -systems.⁶⁷ The conjugation of π -electrons enables efficient absorption of light and subsequent emission of fluorescence. When a COF is excited by



an external light source, such as ultraviolet or visible light, the absorbed energy elevates the π -electrons within the fluorophores to higher energy states. This excitation leads to the formation of an excited state, in which the electrons occupy higher energy levels compared to their ground state configuration. The excited state is transient and unstable, and the electrons tend to return to their ground state through the relaxation processes.⁶⁸ The relaxation process involves the emission of fluorescence, during which the excited electrons release their excess energy in the form of photons. This emission occurs at longer wavelengths than the absorbed light and gives rise to a distinct fluorescence emission spectrum of the COF.⁶⁹ By detecting and recording the emitted photons, fluorescence imaging and analysis can be conducted.⁶⁹ The fluorescence properties of COFs can be influenced by various factors, including the specific fluorophores incorporated into the framework, the size and arrangement of the COF structure, and the surrounding environment.^{69,70} By precisely designing the COF structure and selecting suitable fluorophores, it is possible to customize the fluorescence properties of COFs, such as emission wavelength, quantum yield, and photostability, to meet specific application requirements. It is worth noting that the fluorescence mechanism in COFs can be affected by factors like ACQ or self-quenching, which can reduce the fluorescence intensity.^{71,72} Therefore, strategies aimed at mitigating these effects, such as optimizing the spacing between fluorophores or introducing guest molecules to prevent proximity, are crucial for maximizing the fluorescence efficiency of COFs. In summary, the fluorescence mechanism of COFs involves the excitation of π -electrons within fluorophores, followed by relaxation and emission of fluorescence as the electrons return to the ground state (Fig. 1). A comprehensive understanding of this mechanism enables the rational design and development of fluorescent COFs with enhanced properties for applications in fluorescence imaging and other related fields.⁷³

Bioimaging with bare COFs

On account of extended π -conjugation in many COFs, the materials exhibit fluorescence, so they can directly be used as bioimaging tools. This section discusses the various material design strategies that equip COFs with imaging capabilities.

In a recent study, the potential of TPI-COF as a fluorescent probe for bioimaging was explored. The authors specifically focused on its unique two-photon absorption properties. To investigate its cellular uptake, the researchers employed two-photon confocal laser scanning microscopy (CLSM) and confirmed the internalization of TPI-COF by cells. Interestingly, even when cells were treated with a high concentration of 250 mg mL^{-1} of TPI-COF, they maintained good viability under the 808 nm laser irradiation. The internalization of TPI-COF into 4T1 cells was demonstrated with the COF emitting yellow light upon excitation with a 810 nm laser. It is worth noting that the penetration depth achieved by the two-photon excitation was significantly greater (150 nm) compared to that achieved by the one-photon excitation.⁷²

Another study has demonstrated the benefits of liquid phase exfoliation on the cell internalization of COFs. In this simple method, 1,3,5-triformylglucinol (Tp) and 2,7-diaminopyrene (Py) were used as starting materials to form TpPy COFs (Fig. 2). These COFs were then processed using liquid exfoliation to obtain TpPy covalent organic nanosheets (CONs) with sizes smaller than 200 nm and thicknesses less than 1.7 nm . The resulting TpPy CONs had excellent dispersibility and displayed strong fluorescence and PL properties in aqueous media. They formed highly stable and biocompatible suspensions, which allowed for real-time fluorescence responses and tracking within living organisms. When administered intravenously, TpPy CONs effectively accumulated in tumor tissues by leveraging the enhanced permeability and retention (EPR) effect. This accumulation enabled tumor visualization without the need for labeling or modifying the surface of the CONs. Cell viability tests on MDA-MB-231 and RAW 264.7 cells were performed to study the cytotoxicity of TpPy CONs. The results showed low toxicity, indicating their compatibility with cells. Additionally, CLSM images of cells incubated with TpPy CONs for 24 hours demonstrated clear fluorescence signals without adversely affecting cell activity or causing aggregation within the cytosol. To further investigate the behavior of TpPy CONs in living organisms, *in vivo* fluorescence imaging studies using mice with MDA-MB-231 tumors were performed. Following the intravenous injection of TpPy CONs dispersed in phosphate-buffered saline (PBS), persistent and strong fluorescence signals in the tumor region at various time points (1, 3, 12, and 24 hours post-injection) were observed. Importantly, normal tissues exhibited minimal background signals. These imaging results aligned with biodistribution and histological analyses, confirming the effectiveness of TpPy CONs as bioimaging probes. Overall, this study demonstrates the development of TpPy CONs as a novel two-dimensional nanoplatform suitable for *in vivo* bioimaging applications.⁷⁸

CONs were also prepared from 2,6-diformylpyridine and 4,4',4''-(1,3,5-triazine-2,4,6-triyl)trianiline under microwave irradiation. This COF showcased a hexagonal layered structure, boasting high surface area and thermal stability. Through sonication in water, the bulk COF could be transformed into ultrathin nanosheets. Notably, these exfoliated CONs exhibit improved and blue-shifted photoluminescence compared to their bulk counterpart, attributed to diminished interlayer π - π interactions and an augmented band gap. Intriguingly, researchers explored the biocompatibility and cellular interaction of these COF nanosheets using HeLa cells. Encouragingly, the nanosheets demonstrated non-toxicity and displayed the ability to penetrate the cell nucleus through clathrin-mediated endocytosis within mere 30 minutes. Remarkably, these COF nanosheets emitted strong blue light within the cells, proving effective as label-free nuclear stains for bioimaging purposes.⁷⁹

Aggregation-induced emission fluorogens (AIEgens) with high chemical stability and strong luminescence have been incorporated in COFs for bioimaging. COF TFBE-PDAN was synthesized through a Knoevenagel condensation reaction



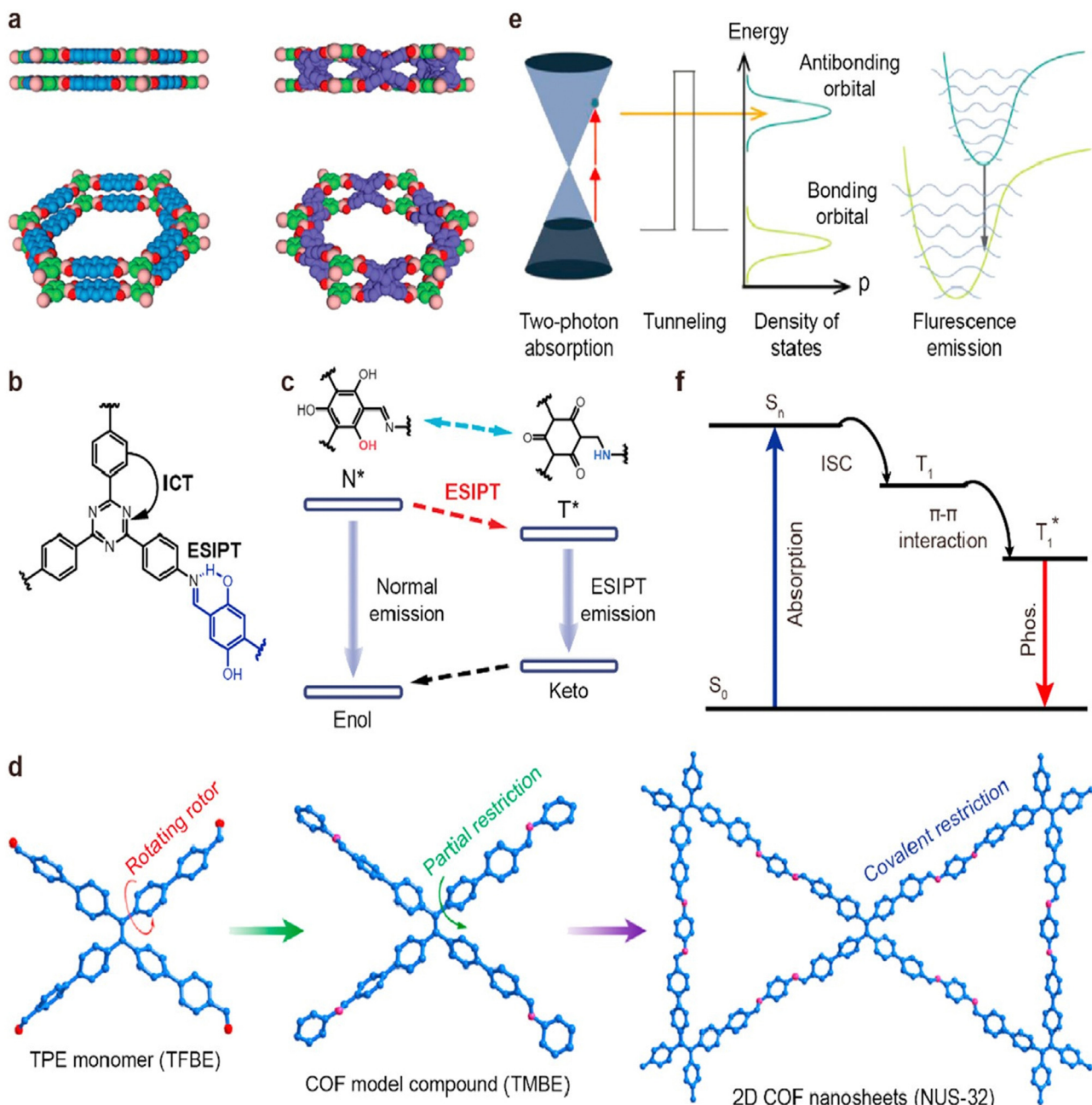


Fig. 1 Mechanisms of luminescent COFs. (a) Excimer (reproduced with permission from the study by Huang *et al.*⁷⁴ Copyright 2015, Wiley-VCH). (b) Intramolecular charge transfer (reproduced with permission from Qian *et al.*⁷⁰ Copyright 2017, American Chemical Society). (c) ESIPT (reproduced with permission from Yin *et al.*⁷⁵ Copyright 2019, The Royal Society of Chemistry). (d) AIE (reproduced with permission from Dong *et al.*⁷⁶ Copyright 2018, American Chemical Society). (e) Two-photon absorption (reproduced with permission from Zeng *et al.*⁴⁴ Copyright 2019, Wiley-VCH). (f) Phosphorescence (adapted with permission from Jin *et al.*⁷⁷ Copyright 2020, Nature Publishing Group). COFs, covalent organic frameworks; ESIPT, excited-state intramolecular proton transfer; and AIE, aggregation-induced emission.

between tetra-(4-aldehyde-(1,1-biphenyl)) ethylene (TFBE) and 1,4-phenylenediacetonitrile (PDAN) under carefully optimized conditions. The incorporation of sp^2 carbon linkages and AIEgen units into COF TFBE-PDAN contributed to its exceptional stability and remarkable luminescent properties. To enhance the capabilities of COFTFBE-PDAN for imaging and ferroptosis in specific tumor cells, tannic acid (TA), a polyphenol derived from plants known for its versatile bonding abilities

and excellent interfacial adhesion characteristics, was introduced. The modification of the COF surface with TA involved interactions such as hydrogen bonding, hydrophobic interactions, and $\pi-\pi$ interactions. In the presence of Fe^{3+} ions, the introduction of TA led to the formation of a network called Fe^{III} TA through coordination-driven cross-linking between metal ions and polyphenols. Remarkably, the Fe^{III} TA network served as a luminescence quencher for COF TFBE-PDAN through

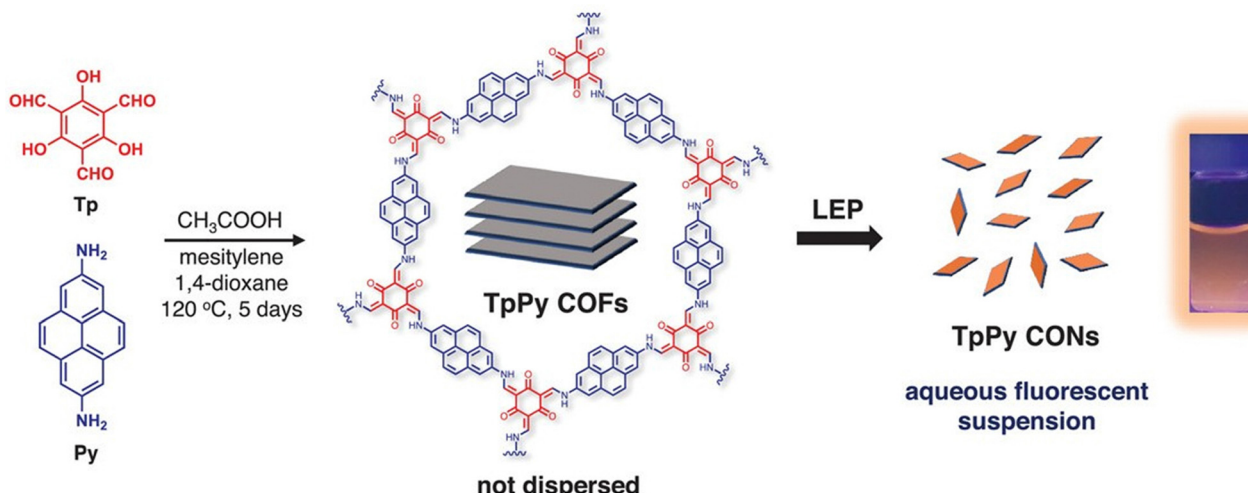


Fig. 2 Schematic diagram of the preparation of TpPy CONs by solvothermal condensation and liquid exfoliation process (fluorescent photograph of a 0.5 mg mL^{-1} TpPy CON dispersion taken under 365 nm UV light). Adapted with permission from ref. 79.

energy transfer, acting as an energy acceptor. The resulting composite, COF TFBE-PDAN@ Fe^{III} TA, was further functionalized with polyethyleneimine (PEI) to introduce tunable positive charges, facilitating its entry into target cells. Within the acidic lysosomes of tumor cells, where the concentration of glutathione (GSH) can be high (up to 10 mM), the Fe^{III} TA network underwent disintegration, releasing Fe^{3+} ions and TA. This disintegration process was facilitated by the combined effect of acidic conditions and high GSH concentration. Disintegration of the Fe^{III} TA coating led to an enhancement of luminescence, thus enabling imaging. The released Fe^{3+} ions could be converted to Fe^{2+} ions within the acidic organelles through the action of GSH and TA. Subsequently, Fe^{2+} ions reacted with the abundant H_2O_2 in tumor cells, generating ROS through the

Fenton reaction. Consequently, GSH levels were significantly depleted, and lipid peroxidation (LPO)-mediated ferroptosis was induced. As the COF's fluorescence was found specifically in the lysosomes, the material was termed a self-reporter for monitoring and visualizing Fe^{III} TA decomposition. To summarize, the COF TFBE-PDAN@ Fe^{III} TA-PEI composite exhibited dual functionality, enabling activatable imaging and induction of ferroptosis in specific tumor cells. The COF-based system displayed strong luminescence emission, which could be activated by the disintegration of the Fe^{III} TA network within the tumor cell microenvironment (Fig. 3). The generation of ROS and depletion of GSH through the composite's action led to ferroptosis, suggesting its potential application in targeted cancer therapy.⁸⁰

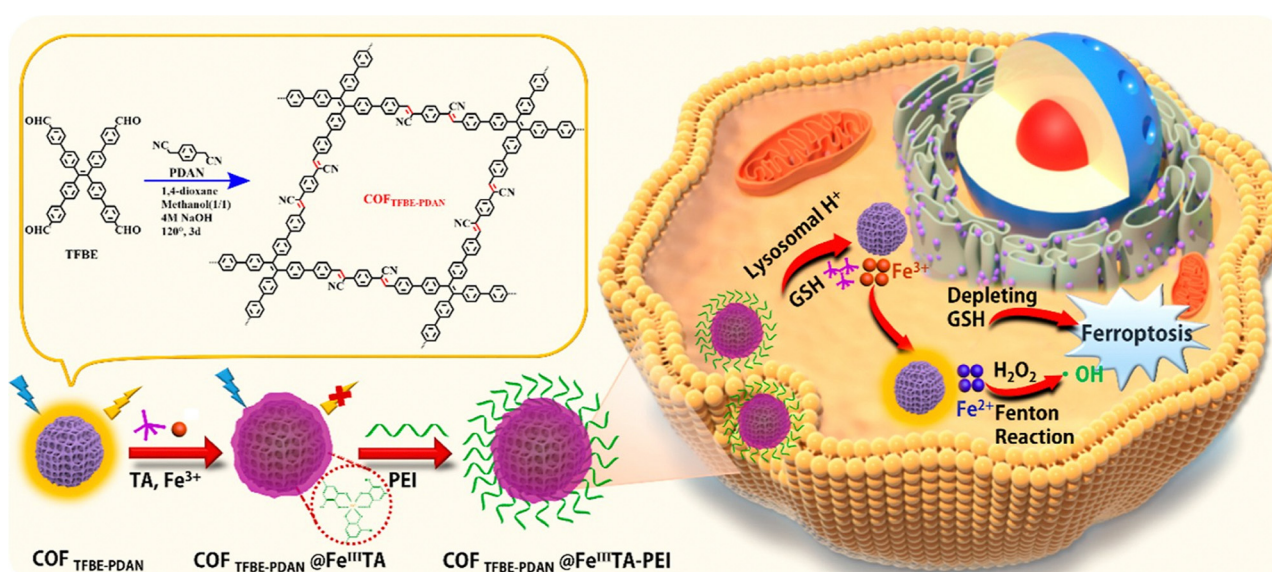


Fig. 3 Schematic illustration of the preparation of COF TFBE-PDAN@ Fe^{III} TA-PEI for luminescence imaging and ferroptosis in target tumor cells. Adapted with permission from ref. 80. Copyright 2022, American Chemical Society.

A series of imine-linked COFs were synthesized for sensing and imaging pH in tumor cells and zebrafish by taking advantage of the reversible imine bond protonation. By combining four different monomers through a condensation reaction, the authors obtained COF₁ to COF₄ with varying pKa values (Fig. 4). These COFs exhibited pH-dependent fluorescence responses, demonstrating their sensitivity compared to the individual building blocks. Among the synthesized materials, COF₂ stood out with its high crystallinity, excellent fluorescence, and suitable pKa for biosensing and bioimaging applications. To enhance its biocompatibility and endocytosis efficiency, COF₂ was modified with poly-D-lysine (PDL). The resulting PDL-modified COF₂ (PDL@COF₂) served as a novel fluorescence probe with a superior linear pH response ranging from 5.0 to 8.0. This pH response was attributed to the reversible protonation and deprotonation properties of PDL@COF₂, and the material was employed as a pH imaging probe in tumor cells and zebrafish. Its environment-sensitive fluorescence allowed for accurate pH imaging in these biological systems. The successful construction of these environment-sensitive fluorescent COFs has significantly expanded the applications of COFs in the field of biology.⁸¹

Researchers also introduced and characterized two innovative 3D sp² carbon-linked COFs, namely JUC-580 and JUC-581, demonstrating their large pores, high stability, and remarkable luminescence properties. Both JUC-580 and JUC-581 exhibited strong fluorescence emissions in the visible range in solid and dispersed states, indicating their potential for applications in fluorescence microscopy and biofluorescence imaging. The study investigated the practical use of JUC-581, one of the 3D COFs, as a carrier for cisplatin, a commonly employed anti-cancer drug. The findings illustrated that JUC-581 proficiently loaded and released cisplatin, serving as an extended fluorescent tracer for monitoring drug transport and cell lysis

processes. Assessment of biocompatibility and cytotoxicity revealed that JUC-581 exhibited good biocompatibility and low cytotoxicity. Conversely, CIS@JUC-581 demonstrated high cytotoxicity, inducing apoptosis in human prostate cancer cells (PC-3). This research broadens the structural diversity of 3D COFs based on different linkages, underscoring their potential applications in biomedicine and fluorescent materials within drug delivery and bioimaging contexts.⁸²

Bioimaging with pore- and surface-functionalized COFs

The rational design of COFs allows for the incorporation of specific functional groups into the pores of the material. These can form non-covalent interactions with small molecules (e.g. therapeutic cargo), or they can be further functionalized with probes, targeting molecules, or inorganic nanoparticles. In this section, we present various examples of COFs that have been post-synthetically modified before being used in bioimaging.

The polymerization of organic ligands within a COF holds promise for enhancing fluorescence properties in bioimaging applications. This approach involves the polymerization of 3,4-ethylenedioxythiophene into a COF (PEDOT@COF) structure. This is an effective tool for fluorescence imaging of Fe³⁺ levels in various biological contexts, including HeLa cells, zebrafish, and mice. Utilizing techniques such as confocal microscopy and live animal imaging, researchers successfully demonstrated the probe's applicability in these settings. The paper also explored the probe's potential for investigating the role of Fe³⁺ in both physiological and pathological diseases. The researchers delve into the regeneration and reuse of the probe through EDTA treatment. The PEDOT@COF probe's fluorescence quenching behavior in the presence of Fe³⁺ is found to be linear within a concentration range of 0–960 μM, boasting a detection limit of 0.82 μM. The fluorescence quenching mechanism is elucidated, involving the inner filter effect (IEF),

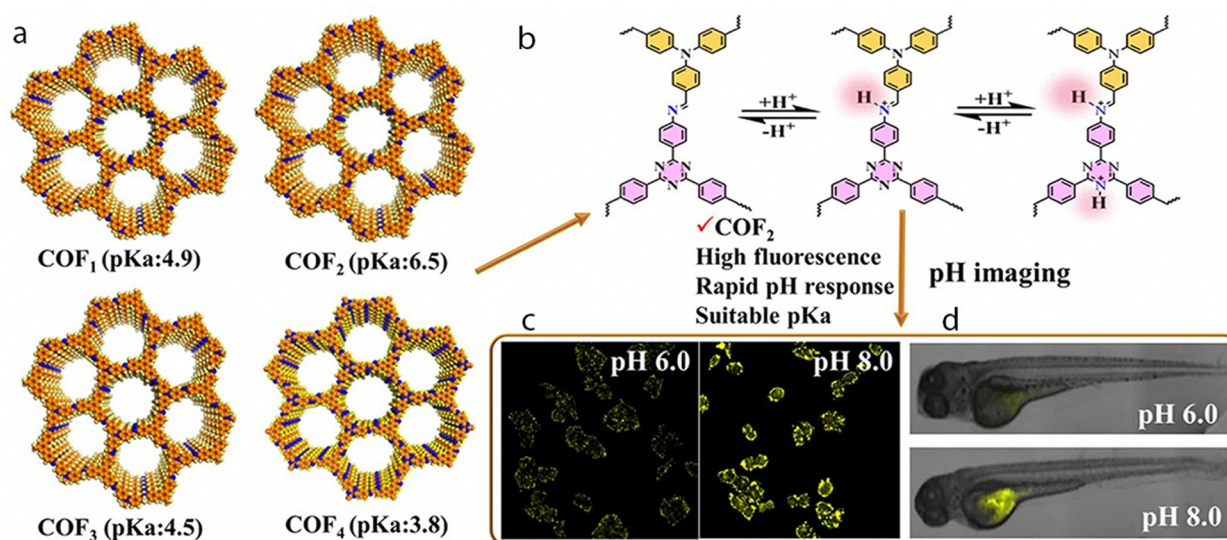


Fig. 4 (a) Schematic illustration of the four COFs (COF₁–COF₄). (b) Protonation/deprotonation of COF₂. Illustration of pH imaging in (c) tumor cells and (d) zebrafish using the pH-responsive PDL@COF₂ nanoprobe. Adapted with permission from ref.81. Copyright 2021, American Chemical Society.



photoinduced electron transfer (PET), and static quenching (SQE) interactions between PEDOT@COF and Fe^{3+} . The study affirms the probe's low toxicity and high biocompatibility, emphasizing its suitability for biological applications.⁸³

An imine-linked TpASH-COF was post-synthetically decorated with 4-amino-1,8-naphthalimide derivative (NPHS), a fluorescent probe capable of emitting two-photon fluorescence upon binding to hydrogen sulfide (H_2S) gasotransmitter. This COF nanoprobe exhibited a remarkable combination of high selectivity and sensitivity for detecting H_2S in live cells and deep tissues, maintaining its effectiveness even in the presence of intracellular enzymes or potential photodegradation. Furthermore, it demonstrated commendable chemical and photostability, low cytotoxicity, and the

ability for long-term tracking. The working principle of the COF nanoprobe involved the formation of reversible chemical bonds between its functional groups and the H_2S gasotransmitter. This interaction induced a change in the electronic properties of the COF, leading to the emission of fluorescence. Upon excitation by a two-photon laser, the COF nanoprobe released fluorescent light, the intensity of which directly reflected the concentration of H_2S in the sample. Its resilience against intracellular enzymes and resistance to photodegradation ensured the precision and reliability of the detection process. Its application in cirrhotic liver models facilitated the monitoring of endogenous H_2S levels, contributing valuable insights to the exploration of its role in liver injury and repair.⁸⁴

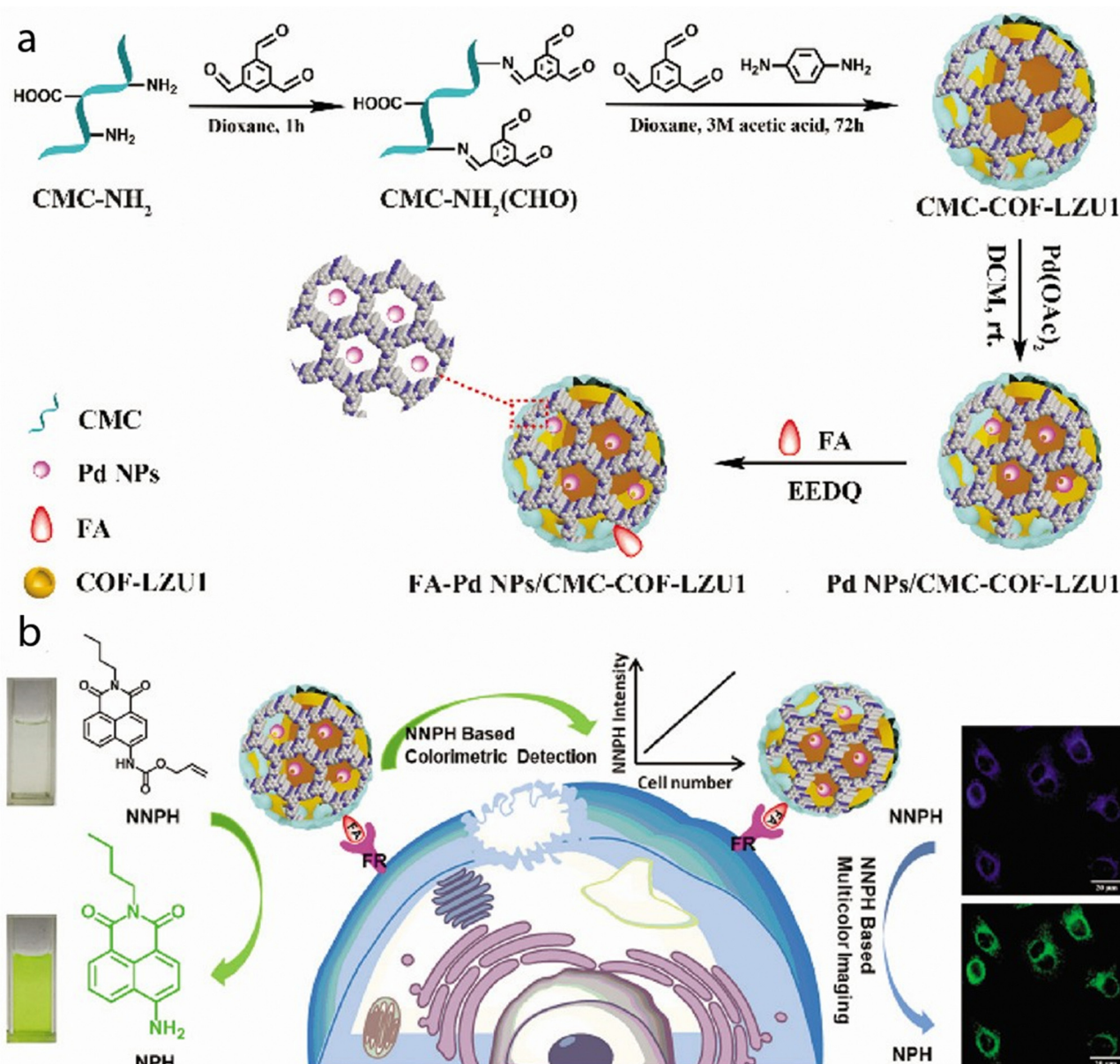


Fig. 5 (a) Illustration of the synthesis process of FA-Pd NPs/CMC-COF-LZU1. (b) Schematic illustration of the dual functions of FA-Pd NPs/CMC-COF-LZU1 for cancer cell imaging. Used with permission of Royal Society of Chemistry from ref. 85; permission conveyed through Copyright Clearance Center, Inc.



Composites made up of organic COFs and inorganic nanoparticle components have been used in bioimaging. A Pd NPs/CMC-COF-LZU1 nanocomposite was prepared by incorporating Pd NPs into a scaffold of carboxymethyl cellulose (CMC)-functionalized COF-LZU1 through *in situ* coordination (Fig. 5). This structural design not only improved the dispersion of the nanocomposite in aqueous solutions, but also enhanced the activity and stability of the Pd NPs. The Pd NPs/CMC-COF-LZU1 nanocomposite exhibited excellent catalytic activity in the cleavage reaction of exogenous *N*-butyl-4-NHAlloc-1,8-naphthalimide (NNPH) to *N*-butyl-4-amido-1,8-naphthalimide (NPH).

This catalytic reaction results in visible changes in both color and fluorescence. The mechanism of this reaction is illustrated in Fig. 5. Furthermore, by modifying the Pd NPs/CMC-COF-LZU1 with folic acid (FA), the resulting FA-modified Pd NPs/CMC-COF-LZU1 nanocomposite can specifically target folate receptor (FR)-positive cancer cells. Upon interaction with these cancer cells, the nanocomposite catalyzes the conversion of NNPH to NPH. This enzymatic reaction leads to a color change and enables multi-color imaging: the blue fluorescence ($\lambda_{\text{em}} = 460 \text{ nm}$) is caused by NNPH, and the green fluorescence ($\lambda_{\text{em}} = 524 \text{ nm}$) is caused by NPH. This innovative strategy utilizing COF-based hybrid materials allows for accurate and sensitive detection and imaging of FR-positive cancer cells.⁸⁵

($\lambda_{\text{em}} = 524 \text{ nm}$) is caused by NPH. This innovative strategy utilizing COF-based hybrid materials allows for accurate and sensitive detection and imaging of FR-positive cancer cells.⁸⁵

Spherical nucleic acids hold great potential in nanomedicine, specifically the detection of biomarkers, but their incorporation into nanomaterials such as COFs is challenging due to limited methods for functionalizing COFs. To address this, a bonding defect-amplified modification (BDAM) strategy for the facile preparation of functionalized COFs has been proposed. In the BDAM strategy, poly(acrylic acid) was used as a defect amplifier to modify the surface of COF nanoparticles. By forming amide bonds with unreacted amino residues of COFs, poly(acrylic acid) converted and amplified these residues into abundant reactive carboxyl groups. This modification created a platform for further functionalization of the COF nanoparticles. Amino group terminal-decorated hairpin DNA was densely grafted onto the surface of the COF nanoparticles, resulting in the formation of a spherical nucleic acid probe (SNAP; Fig. 6). Experimental validation confirmed the successful preparation of the COF-based SNAP, which demonstrated the ability to specifically detect and illuminate RNA biomarkers

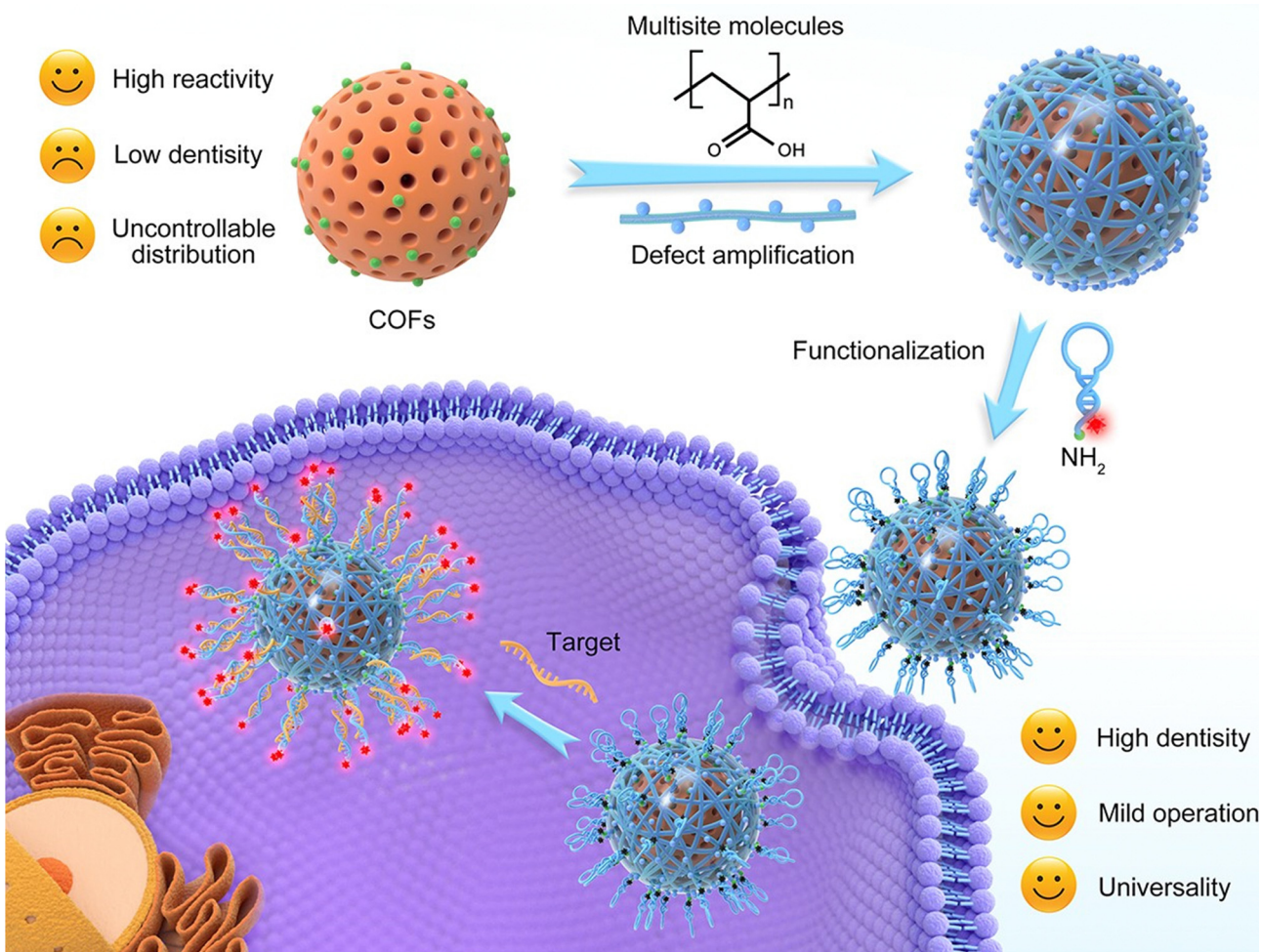


Fig. 6 Schematic illustration of the preparation of the COF-based SNAP with a bonding defect-amplified modification strategy and its application for cancer cell imaging. Adapted with permission from ref. 86. Copyright 2021, American Chemical Society.



in living cells for cancer diagnostic imaging. Overall, the COF-based SNAP showed promise for biomedical applications, particularly in cancer diagnosis. The proposed BDAM strategy offers a useful approach for preparing functionalized COFs that can be extended to diverse fields of research and technology.⁸⁶

A tricolor fluorescent nanoprobe was designed for simultaneous imaging of biomarkers with different spatial distributions in living cells. The COF NPs were prepared from polycondensation of 1,3,5-tris(4-aminophenyl) benzene and 2,5-dimethoxyterephthaldehyde (Fig. 7). The nanoprobe consisted of a ~80 nm fluorescent COF that emitted light near 510 nm. The two functional nucleic acids, a Cy5-labeled MUC1 aptamer and a TAMRA-labeled survivin mRNA antisense nucleotide, were grafted onto the COF nanoparticles using a freezing method to enhance the interaction between the COF NPs and the nucleic acids, thus improving detection performance. The nanoprobe demonstrates high specificity and recovers its fluorescence signal only when it encounters the specific targets. Additionally, the intrinsic fluorescence of the COF allows real-time visualization of cellular uptake and intracellular distribution of the nanoparticles. This enabled successful visualization of the MUC1 protein in the cellular membrane and survivin mRNA in the cytoplasm of cancerous cells. Normal cells showed low expression levels of these biomarkers, so no significant fluorescence signal was observed. Interestingly, the tricolor nanoprobe was used to visualize the upregulation of

oligonucleotide, were grafted onto the COF nanoparticles using a freezing method to enhance the interaction between the COF NPs and the nucleic acids, thus improving detection performance. The nanoprobe demonstrates high specificity and recovers its fluorescence signal only when it encounters the specific targets. Additionally, the intrinsic fluorescence of the COF allows real-time visualization of cellular uptake and intracellular distribution of the nanoparticles. This enabled successful visualization of the MUC1 protein in the cellular membrane and survivin mRNA in the cytoplasm of cancerous cells. Normal cells showed low expression levels of these biomarkers, so no significant fluorescence signal was observed. Interestingly, the tricolor nanoprobe was used to visualize the upregulation of

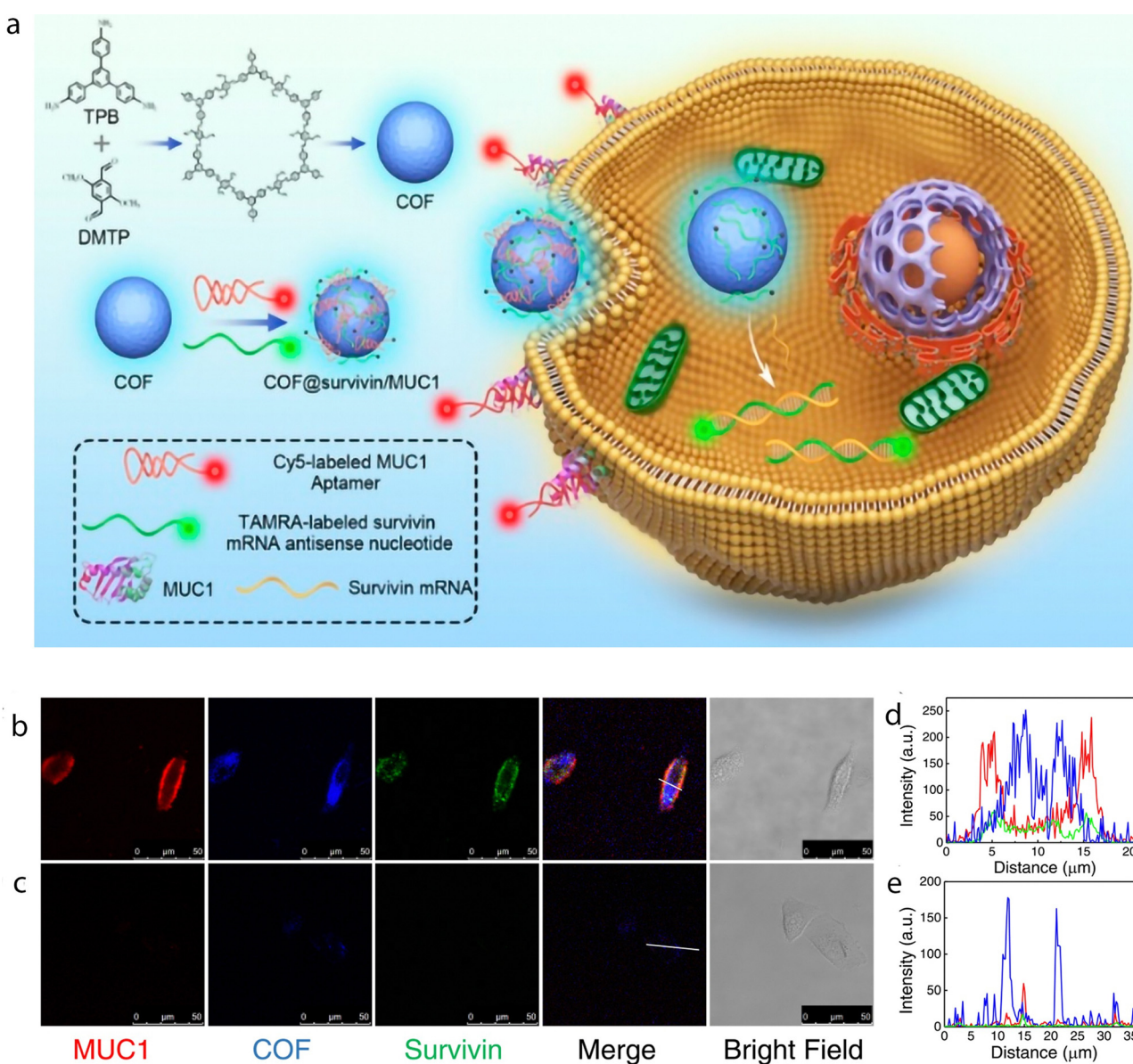


Fig. 7 Monitoring cancer exosomes infecting normal cells using the nanoprobe. (a) Schematic illustration of the synthesis of a COF and the multicolor nanoprobe and its application for cell imaging. Confocal imaging of MCF-10A cells with (b) or without (c) preincubation with the culture medium containing cancer cell exosomes. (d) and (e) Alterations of fluorescence intensities of different signals in the labeled regions of cells in (b) and (c), respectively. Adapted with permission from ref. 87.



survivin mRNA and MUC1 in normal cells after infection with cancer cell exosomes. This COF-based multicolor nanoprobe offers a valuable tool for simultaneous imaging of biomarkers located in different cellular compartments. By quenching fluorescence signals of dye-labeled nucleic acids with the COF NPs and restoring the signals upon binding to their respective targets, distinct spatial imaging of biomarkers was achieved. This study not only expands the application of nanoscale COFs but also provides insights for the rational design of COF-based nanoprobe for bioanalysis.⁸⁷

The cellular condition of hypoxia, or low oxygen levels, was imaged using a fluorescent β -ketoenamine COF post-synthetically modified with a nitroimidazole target compound (Fig. 8). Nitroimidazole derivatives are known for their ability to act as hypoxia markers, undergoing bioreductive activation and selectively accumulating in hypoxic cells. The resulting nitroimidazole COF (NI-COF) is stable under physiological conditions, could be exfoliated to achieve a particle size of ~ 160 nm, and possessed favorable fluorescence properties with an emission peak at 480 nm upon excitation at 420 nm under both neutral and slightly acidic conditions. These properties are advantageous for imaging hypoxic conditions, as the tumor microenvironment often exhibits acidic pH levels. Importantly, the NI-COF exhibited low cytotoxicity, making it suitable for use as a fluorescence imaging tool. The fluorescence microscopy images clearly showed that the NI-COF preferentially accumulated in HeLa cells incubated under hypoxic conditions compared to those incubated under normoxic conditions. This

selective accumulation of the NI-COF in hypoxic cells validated its potential as a fluorescence imaging probe for hypoxia. This tool holds promise for further investigations and applications in the field of hypoxia imaging.⁸⁸

Researchers introduced an innovative nanoreactor designed for *in vivo* ATP detection and imaging. This nanoreactor, known as h-CCS, encapsulated a CRISPR/Cas12a system and an ATP aptamer within a hollow COF. Comprising the CRISPR-Cas12a system, a fluorophore quencher-labeled ssDNA substrate (ssDNA-FQ), and a DNA activator pre-hybridized with the ATP aptamer, the CRISPR/Cas12a sensor operated by inhibiting trans-cleavage activity when the DNA activator was hybridized with the ATP aptamer. Because of the presence of ATP, the DNA activator was released, activating Cas12a and generating a fluorescence signal by cleaving the ssDNA reporter. The incorporation of this sensor into a hollow COF, synthesized using amorphous ZIF-8 as a template, enhanced its stability *in vivo* and allowed ATP-induced fluorescence for imaging. This hollow COF safeguarded the sensor from external interferences, such as DNase I and proteinase K, and facilitated cellular uptake and mitochondrial localization of the sensor. Furthermore, its ATP-responsive performance was showcased in living cells and mice, effectively distinguishing cancer cells with elevated ATP levels, emitting stronger fluorescence signals, from healthy cells with lower ATP levels, exhibiting weaker or no fluorescence. This strategy not only expands the applications of CRISPR-Cas systems but also holds promise for diverse proteins within porous matrices, opening avenues for

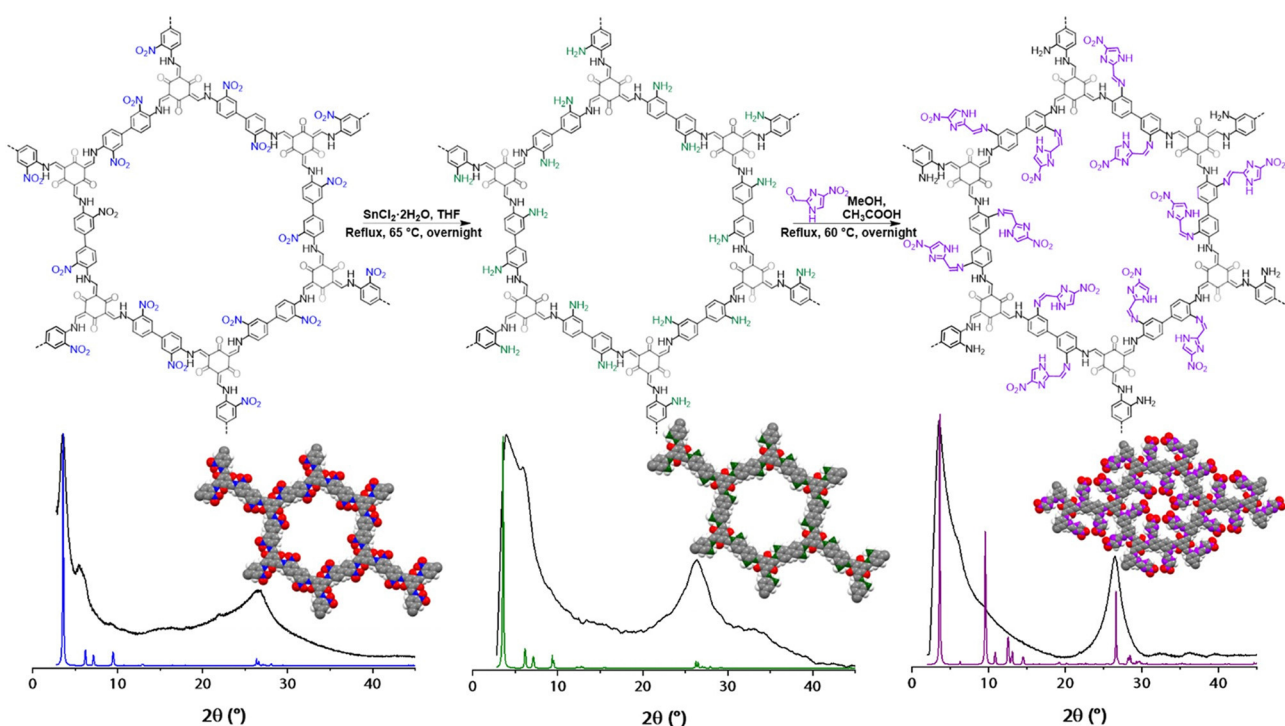


Fig. 8 Synthetic procedure for the preparation of NI-COF for hypoxia imaging. The parent NO₂-COF was reduced into NH₂-COF, and a nitroimidazole moiety was conjugated to afford NI-COF. The corresponding experimental and simulated PXRD patterns of the three COFs are also shown. Reproduced from ref. 88. Permission not required.



application in clinical diagnostics, medical research, and biomimetic nanodevices.⁸⁹

Researchers also devised two nanoprobe engineered for the concurrent identification and imaging of two tumor-associated mRNAs (survivin and TK1) within living cells. The nanoprobe, utilizing COFs and integrating dye-labeled DNA sequences specific to the target mRNAs, functioned through a nucleic acid-specific “off-on” mechanism. Porphyrin-based COFs, with their broad-spectrum absorption capabilities, acted as quenchers for dye-labeled single-stranded DNAs (ssDNAs) targeting tumor-associated mRNAs. Employing a freezing method, the researchers loaded dye-labeled ssDNAs onto the COF NPs, enhancing the interaction and quenching effect between the COF NPs and the ssDNAs. The COF-DNA bicolor probes adeptly entered living cells, selectively binding to overexpressed target mRNAs such as survivin and TK1 in cancer cells. Upon binding to the target mRNAs, the dye-labeled ssDNAs were released from the COF NPs, restoring their fluorescence signals and enabling the simultaneous imaging of dual mRNAs in living cells. The freezing-method-prepared nanoprobe, designed to enhance DNA loading capacity and fluorescence quenching, exhibited elevated signal intensities in cells with heightened expression of the target mRNAs. In contrast, it maintained comparable signals in cells with lower target expression. The development of high-performance COF-based nanoprobe for the detection of multiple biomarkers also introduces a promising tool for enhanced cancer diagnostic imaging.⁹⁰

COFs for combined bioimaging and therapy

The development of advanced materials for biomedical applications has led to the exploration of innovative strategies for combining diagnostic imaging with therapeutic interventions. The unique advantage of fluorescent COFs lies in their seamless integration of imaging and therapy. By incorporating therapeutic agents into the COF structure while retaining their fluorescence properties, these materials enable real-time monitoring of drug delivery and therapeutic responses. This integration enhances treatment precision, reduces treatment-associated risks, and provides critical insights into the therapeutic process. In conclusion, fluorescent COFs represent an exciting advancement in biomedical research, offering a versatile platform for combined imaging and therapy. As research in this field continues to evolve, fluorescent COFs are poised to play a pivotal role in revolutionizing the diagnosis and treatment of diseases, ushering in a new era of precision medicine.

A COF that exhibited deep blue emission in polar solvents was loaded with a common anticancer drug doxorubicin (Dox) with a green emission. Through abundant H-bonding and π - π interactions, Dox was successfully loaded onto the COF, forming a fluorescence resonance energy transfer (FRET) system that effectively quenched the emission of Dox. The drug loading ratio achieved was 35%, and approximately 85% of the drug was released under acidic conditions mimicking the tumor microenvironment. This release was primarily attributed to the protonation of the amino groups in Dox, which disrupted the

H-bonding with the COF. CLSM imaging results indicated that after 1 hour of incubation, a small amount of the drug was released, primarily in the cytoplasm with weak emission. However, after 4 hours, significant fluorescence was observed in both the cytoplasm and the nucleus, indicating successful cellular uptake and subsequent intracellular drug release.⁹¹

A slightly more complex smart nanosystem based on a COF for simultaneous biomarker imaging and cancer microenvironment-responsive chemotherapy has also been developed. The system utilized porphyrin COF NPs as carriers for the model drug Dox and Cy5-labeled single-stranded DNA (ssDNA) for recognizing thymidine kinase 1 (TK1) mRNA (Fig. 9). The adsorption of ssDNA onto Dox-loaded COF NPs quenched the Cy5 fluorescence through energy transfer, which could be restored upon specific binding to TK1 mRNA. Interestingly, incorporating Dox within ssDNA improved fluorescence quenching efficiency, and the COF NPs prevented nonspecific drug release. This resulted in a low fluorescence signal and reduced toxicity in normal cells. In cancer cells, the overexpression of TK1 mRNA and the acidic microenvironment led to an intense fluorescence signal and drug release. Thus, the COF-based nanosystem enabled specific imaging of TK1 mRNA as a cancer biomarker and triggered drug release in the tumor microenvironment.⁸⁷

In addition to combining bioimaging with chemotherapy, integration of imaging with photodynamic therapy (PDT) has also been investigated. A nanoplatform was composed of a core made of lanthanide-doped upconversion nanoparticles (UCNPs), onto which COFs with different shell thicknesses were deposited through a process called core-mediated imine polymerization (UCCOFs; Fig. 10). By carefully adjusting the thickness of the COF shell, the PDT effectiveness of the UCCOFs is significantly improved by achieving a 12.5-fold enhancement compared to pristine COFs. The UCNPs core's unique properties of being excited by NIR light and emitting light of shorter wavelength allowed for efficient PDT when tested in living organisms. The production of ROS during PDT was tracked by loading indocyanine green (ICG), a ROS indicator, onto the UCCOFs, creating UCCOFs-1. Under NIR light irradiation at 980 nm, UCCOFs-1 emitted strong light at 541 nm and at 654 nm, which triggered the PDT process. As the PDT progressed, the loaded ICG gradually broke down due to the presence of singlet oxygen (${}^1\text{O}_2$). This breakdown activated luminescence at 800 nm from UCCOFs-1, allowing the authors to monitor the location and amount of ${}^1\text{O}_2$ being generated in real-time within a living organism.

Consequently, the intensity of luminescence from UCCOFs-1 showed a direct relationship with the treatment outcomes, enabling immediate prediction of the therapeutic effects. This capability is valuable for tailoring the treatment schedule to each individual, minimizing the risk of overtreatment, and reducing side effects. Through the use of COFs with high porosity and incorporation of ICG, upconverting COF nanoplatforms demonstrated efficient PDT capabilities while also providing the means to monitor the therapeutic process. The nanoplatform's ability to self-report the location and quantity of ${}^1\text{O}_2$ through NIR-activated upconversion luminescence



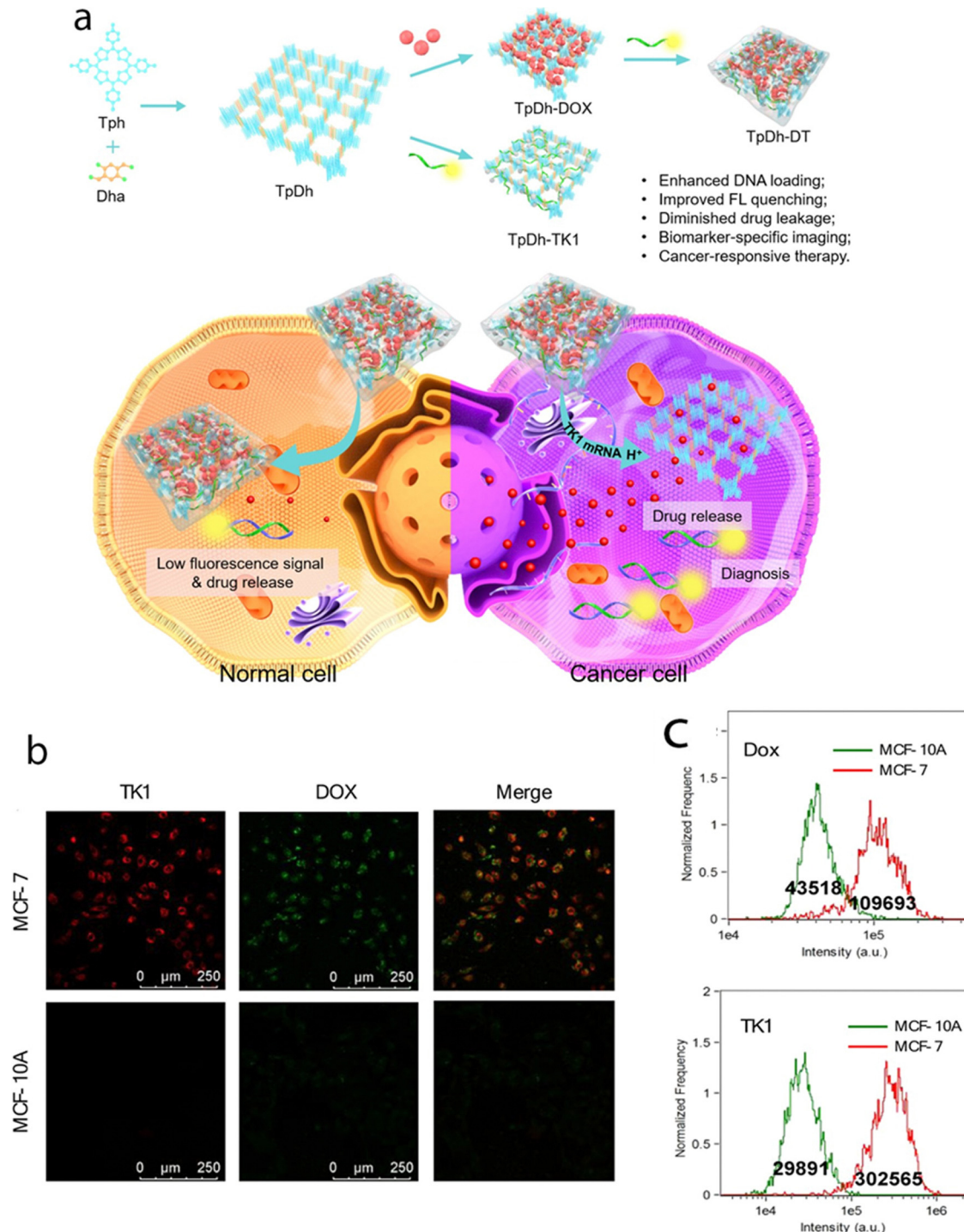


Fig. 9 (a) Schematic illustration of the preparation, cancer cell specific imaging, and therapeutic applications of TpDh-DOX. (b) Confocal images of MCF-7 and MCF-10A cells treated with TpDh-DOX. (c) Flow cytometry analysis and average fluorescence intensities of TK1(Cy5) and Dox in MCF-7 and MCF-10A cells after treatment with TpDh-DOX. Adapted with permission from ref. 91. Copyright 2021, American Chemical Society.

during *in vivo* PDT holds promise for predicting therapeutic effects on time.⁹²

Challenges and future prospectives

The large-scale manufacture of COFs with desired functionalities is a challenging yet essential prerequisite for their practical

applications in bioimaging, particularly in clinical settings. While significant progress has been made in the laboratory-scale design and synthesis of COFs, achieving uniformity and reproducibility in scale-up production presents considerable difficulties. During the synthesis and subsequent processes, COFs are susceptible to aggregation, dissolution, or reactions

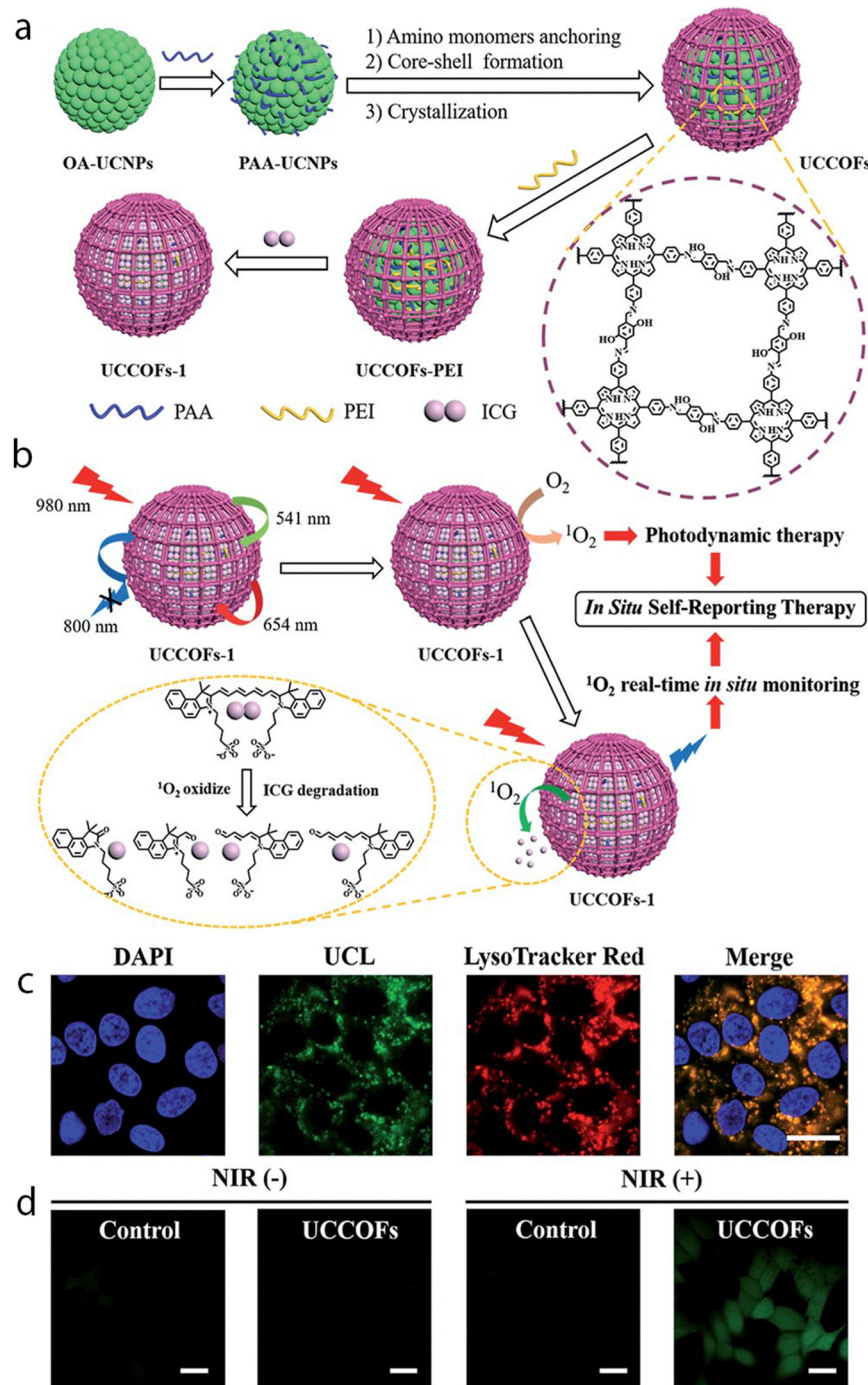


Fig. 10 (a) A schematic illustration showing the design and synthesis of the upconverting COF nanoplateform UCCOFs-1. (b) A schematic illustration of the NIR-excited *in situ* self-reporting PDT process. (c) Confocal fluorescence images of HeLa cells treated with UCCOFs; scale bar: 20 μm . (d) Intracellular $^{1}\text{O}_2$ production with or without NIR irradiation determined via a H2DCFH-DA assay; scale bar: 20 μm . Reproduced from ref. 92 with permission from the Royal Society of Chemistry.

that reduce surface energy.⁹³ These transformations may lead to significant changes in shape, volume, mechanical properties, and permeability, potentially undermining the pre-designed functions of COFs. These challenges are particularly pronounced when dealing with new categories of fluorescent COFs.

Fluorescent COFs have a lot of potential for bioimaging, but there are some challenges we need to tackle in this field. One of

the main challenges is making sure that fluorescent COFs work effectively in living cells. It is really important to carefully study how they affect cell health and function. Researchers have to check for any potential harm and find ways to minimize negative impacts on cell morphology and function. We also need to make sure that fluorescent COFs stay stable in the body's natural conditions, so we can rely on them for imaging

over a long time. It is essential to maintain their ability to emit fluorescence over extended periods. Coming up with strategies to improve their stability against degradation is a big challenge that needs a lot of thought. Another challenge is imaging deep tissues and organs. Light scattering and absorption in biological tissues make it difficult for fluorescence signals to penetrate deeply. We need to find ways to overcome this and develop techniques that allow us to see deeper structures. Finally, achieving high specificity and selectivity in bioimaging is crucial for accurately detecting specific cells or biomolecules. Designing fluorescent COFs that bind specifically to desired targets while minimizing interactions with other substances is quite challenging. Overall, addressing these challenges will help us unlock the full potential of fluorescent COFs for bioimaging, advancing our understanding of cellular processes and diseases.

In the future, researchers should focus on integrating multiple functions into fluorescent COFs to expand their applications in bioimaging. By incorporating various imaging probes, such as different fluorophores or contrast agents, into a COF structure, it will be possible to simultaneously image multiple targets or biomarkers. This multifunctionality will provide a comprehensive understanding of cellular processes and facilitate a deeper exploration of complex biological systems. Researchers need to focus on enhancing the biocompatibility and stability of fluorescent COFs under physiological conditions. This involves ensuring that COFs retain their structural integrity and aqueous stability, especially when interacting with biological systems. Future studies should delve into more intricate biodistribution analyses, considering diverse administration routes, various time points, and potential deviations under distinct physiological conditions. Extensive investigations over extended periods are imperative to gauge the stability of COFs, unraveling their biodegradation patterns and potential enduring impacts. In-depth exploration into the mechanisms of biotoxicity is essential, scrutinizing specific cellular pathways, potential inflammatory responses, and prolonged effects on cell health. Researchers ought to explore optimal size and shape configurations that optimize biocompatibility, considering cellular uptake mechanisms and potential influences on physiological processes. A concerted effort should be made to tailor the surface chemistry of COFs, enhancing biocompatibility, mitigating immune responses, and refining interactions with biological components. Investigating the integration of various imaging modalities within COFs is paramount, paving the way for comprehensive imaging with heightened specificity and sensitivity. Targeted imaging plays a vital role in bioimaging as it enables specific visualization of particular cells, organelles, or biomolecules. Scientists are actively investigating the integration of targeting ligands, such as antibodies or aptamers, onto the surface of COFs to achieve selective imaging. This approach will allow precise detection of disease-related biomarkers, contributing to early diagnosis and personalized medicine. The translation of fluorescent COFs from *in vitro* to *in vivo* imaging shows great promise. Researchers are striving to overcome the limitations

posed by light penetration and tissue autofluorescence by developing NIR-emissive COFs. These can penetrate deeper into tissues and provide reduced background noise, enabling non-invasive and real-time imaging of living organisms. This advancement paves the way for non-invasive and real-time imaging of living organisms, expanding the potential of COFs in the realm of *in vivo* diagnostics. There is a need for collaboration between researchers from different disciplines. Interdisciplinary efforts can bring together expertise in chemistry, materials science, biology, and medicine to address multifaceted challenges and drive innovation in bioimaging applications.

The combination of bioimaging capabilities with therapeutic functionalities within COFs is an emerging research area. By incorporating drug molecules or therapeutic agents into COFs, scientists can create theranostic platforms that allow simultaneous imaging and targeted therapy. The imaging capabilities of COFs will enable real-time monitoring of therapeutic responses, facilitating the optimization of treatment strategies and ultimately improving patient outcomes. This dynamic feedback loop holds the potential to optimize treatment strategies, leading to improved patient outcomes.

In conclusion, addressing challenges related to biocompatibility, stability, specificity, imaging depth, and *in vivo* performance is crucial for the successful application of fluorescent COFs in bioimaging. It requires a multidisciplinary approach involving materials science, biology, medicine, and imaging technology. Overcoming these challenges will unlock the full potential of fluorescent COFs and pave the way for their widespread use in advancing our understanding of cellular processes and disease states. Fluorescent COFs for bioimaging are exciting and hold great potential for advancing our understanding of biological systems, diagnosing diseases, and developing personalized medicine. Continued research and innovation in this field will undoubtedly lead to transformative applications in biomedical imaging.

Author contributions

All authors contributed equally.

Conflicts of interest

The authors declare no conflict of interest.

Acknowledgements

CSK acknowledges the Shetty research group and Khalifa University Abu Dhabi for hosting, and JSSSTU for facilitating his research visit. DS acknowledges the resource support under the Center for Catalysis and Separations (CeCaS, grant RC2-2018-024). T.S. acknowledges financial support from the Slovenian Research Agency (research core funding No. P2-0412).



References

- 1 K. D. Wegner and N. Hildebrandt, *Chem. Soc. Rev.*, 2015, **44**, 4792–4834.
- 2 G. Yang, *Wiley Interdiscip. Rev.: Syst. Biol. Med.*, 2013, **5**, 367–380.
- 3 K. B. Busi, S. Das, M. Palanivel, K. K. Ghosh, B. Gulyás, P. Padmanabhan and S. Chakrabortty, *Nanomaterials*, 2023, **13**(3), 529.
- 4 S. Yao, X. Zhao, X. Wang, T. Huang, Y. Ding, J. Zhang and L. Li, *Adv. Mater.*, 2022, **34**, 2109568.
- 5 S. Fernandes, G. Williams, E. Williams, K. Ehrlich, J. Stone, N. Finlayson and K. Dhaliwal, *Eur. Respir. J.*, 2020, **57**, 2002537.
- 6 M. Donaldson, J. Pulido, B. Mullan, D. Inwards, H. Cantrill, M. Johnson and M. Han, *Clin. Experiment. Ophthalmol.*, 2006, **34**, 846–851.
- 7 F. Carty, C. Shortt, M. Shelly and S. Eustace, *Seminars in Musculoskeletal Radiology*, 2010, **14**(01), 068–085.
- 8 C. Spiek, K. Herrmann and J. Czernin, *J. Nucl. Med.*, 2016, **57**(3), 420–430.
- 9 M. Chen and M. Yin, *Prog. Polym. Sci.*, 2014, **39**, 365–395.
- 10 Y. Chen, S. Wang and F. Zhang, *Nat. Rev. Bioeng.*, 2023, **1**, 60–78.
- 11 S. Yang, X. Tan, L. Tang and Q. Yang, *Front. Chem.*, 2021, **9**, 763495.
- 12 Y. Chen, B. Sun, X. Jiang, Z. Yuan, S. Chen, P. Sun, Q. Fan and W. Huang, *J. Mater. Chem. B*, 2021, **9**, 1002–1008.
- 13 H. H. Han, H. Tian, Y. Zang, A. C. Sedgwick, J. Li, J. L. Sessler, X. P. He and T. D. James, *Chem. Soc. Rev.*, 2021, **50**, 9391–9429.
- 14 G. Hong, A. L. Antaris and H. Dai, *Nat. Biomed. Eng.*, 2017, **1**, 10.
- 15 Y. Li, Q. Chen, X. Pan, W. Lu and J. Zhang, *Top. Curr. Chem.*, 2022, 380.
- 16 F. Ding, Y. Fan, Y. Sun and F. Zhang, *Adv. Healthcare Mater.*, 2019, **8**.
- 17 Y. Jiao, K. Liu, G. Wang, Y. Wang and X. Zhang, *Chem. Sci.*, 2015, **6**, 3975–3980.
- 18 J. O. Escobedo, O. Rusin, S. Lim and R. M. Strongin, *Curr. Opin. Chem. Biol.*, 2010, **14**, 64–70.
- 19 Z. Kam, E. Zamir and B. Geiger, *Trends Cell Biol.*, 2001, **11**, 329–334.
- 20 G. Hong, J. T. Robinson, Y. Zhang, S. Diao, A. L. Antaris, Q. Wang and H. Dai, *Angew. Chem., Int. Ed.*, 2012, **51**, 9818–9821.
- 21 Q. Yang, Z. Ma, H. Wang, B. Zhou, S. Zhu, Y. Zhong, J. Wang, H. Wan, A. Antaris, R. Ma, X. Zhang, J. Yang, X. Zhang, H. Sun, W. Liu, Y. Liang and H. Dai, *Adv. Mater.*, 2017, **29**.
- 22 A. L. Antaris, H. Chen, K. Cheng, Y. Sun, G. Hong, C. Qu, S. Diao, Z. Deng, X. Hu, B. Zhang, X. Zhang, O. K. Yaghi, Z. R. Alamparambil, X. Hong, Z. Cheng and H. Dai, *Nat. Mater.*, 2016, **15**, 235–242.
- 23 M. Bruchez, M. Moronne, P. Gin, S. Weiss and A. P. Alivisatos, *Science*, 1998, **281**, 2013–2016.
- 24 X. Gao, Y. Cui, R. M. Levenson, L. W. K. Chung and S. Nie, *Nat. Biotechnol.*, 2004, **22**, 969–976.
- 25 M. L. Liu, B. B. Chen, C. M. Li and C. Z. Huang, *Green Chem.*, 2019, **21**, 449–471.
- 26 X. Michalet, F. F. Pinaud, L. A. Bentolila, J. M. Tsay, S. Doose, J. J. Li, G. Sundaresan, A. M. Wu, S. S. Gambhir and S. Weiss, *Vivo Imaging Diagn.*, 2005, **307**, 538–544.
- 27 J. T. Robinson, G. Hong, Y. Liang, B. Zhang, O. K. Yaghi and H. Dai, *J. Am. Chem. Soc.*, 2012, **134**, 10664–10669.
- 28 R. Weissleder, *Nat. Biotechnol.*, 2001, **19**, 316–317.
- 29 W. R. Zipfel, R. M. Williams and W. W. Webb, *Nat. Biotechnol.*, 2003, **21**, 1369–1377.
- 30 Y. Zhou, X. Liang and Z. Dai, *Nanoscale*, 2016, **8**, 12394–12405.
- 31 Y. Liu, Z. Yang, X. Huang, G. Yu, S. Wang, Z. Zhou, Z. Shen, W. Fan, Y. Liu, M. Davisson, H. Kalish, G. Niu, Z. Nie and X. Chen, *ACS Nano*, 2018, **12**, 8129–8137.
- 32 Y. Hama, Y. Urano, Y. Koyama, P. L. Choyke and H. Kobayashi, *Biochem. Biophys. Res. Commun.*, 2006, **348**, 807–813.
- 33 P. J. Fenton, *Br. J. Ophthalmol.*, 1965, **49**, 205–208.
- 34 O. O. Abugo, R. Nair and J. R. Lakowicz, *Anal. Biochem.*, 2000, **279**, 142–150.
- 35 R. Tong and J. Cheng, *J. Am. Chem. Soc.*, 2009, **131**, 4744–4754.
- 36 Y. Zhang, Y. Li, J. Ma, X. Wang, Z. Yuan and W. Wang, *Nano Res.*, 2018, **11**, 4278–4292.
- 37 H. Wang, P. Zhao, X. Liang, X. Gong, T. Song, R. Niu and J. Chang, *Biomaterials*, 2010, 4129–4138.
- 38 P. Horcajada, T. Chalati, C. Serre, B. Gillet, C. Sebrie, T. Baati, J. F. Eubank, D. Heurtaux, P. Clayette, C. Kreuz, J. S. Chang, Y. K. Hwang, V. Marsaud, P. N. Bories, L. Cynober, S. Gil, G. Férey, P. Couvreur and R. Gref, *Nat. Mater.*, 2010, **9**, 172–178.
- 39 S. Y. Ding and W. Wang, *Chem. Soc. Rev.*, 2013, **42**, 548–568.
- 40 A. Esrafil, A. Wagner, S. Inamdar and A. P. Acharya, *Adv. Healthcare Mater.*, 2021, **10**, 54.
- 41 M. Fernández-Suárez and A. Y. Ting, *Nat. Rev. Mol. Cell Biol.*, 2008, **9**, 929–943.
- 42 A. Jayagopal, P. K. Russ and F. R. Haselton, *Bioconjugate Chem.*, 2007, **18**, 1424–1433.
- 43 C. S. Ke, C. C. Fang, J. Y. Yan, P. J. Tseng, J. R. Pyle, C. P. Chen, S. Y. Lin, J. Chen, X. Zhang and Y. H. Chan, *ACS Nano*, 2017, **11**, 3166–3177.
- 44 E. Petryayeva, W. R. Algar and I. L. Medintz, *Appl. Spectrosc.*, 2013, **67**, 215–252.
- 45 C. Liao and S. Liu, *J. Mater. Chem. B*, 2021, **9**, 6116–6128.
- 46 Y. Shi, J. Yang, F. Gao and Q. Zhang, *ACS Nano*, 2023, **17**, 1879–1905.
- 47 S. Liang, M. H. Li, M. Qi, L. Wang and Y. W. Yang, *Chem. Mater.*, 2023, **35**, 8353–8370.
- 48 A. Mal, H. Ding, M. Li and W. Li, *ACS Appl. Nano Mater.*, 2022, **5**, 13972–13984.
- 49 N. Singh, S. Son, J. An, I. Kim, M. Choi, N. Kong and J. S. Kim, *Chem. Soc. Rev.*, 2021, **50**, 12883–12896.
- 50 Y. Liu, Y. Zhang, X. Li, X. Gao, X. Niu, W. Wang and Z. Yuan, *Nanoscale*, 2021, **11**, 10429–10438.



51 A. R. Bagheri, C. Li, X. Zhang, X. Zhou, N. Aramesh, H. Zhou and J. Jia, *Biomater. Sci.*, 2021, **9**, 5745–5761.

52 C. Valenzuela, C. Chen, M. Sun, Z. Ye and J. Zhang, *J. Mater. Chem. B*, 2021, **9**, 3450–3483.

53 S. Yao, M. Zheng, S. Wang, T. Huang, Z. Wang, Y. Zhao and L. Li, *Adv. Funct. Mater.*, 2022, **32**, 2209142.

54 S. Yao, Z. Liu and L. Li, *Nano-Micro Lett.*, 2021, **13**, 176.

55 S. Yao, Z. Wang and L. Li, *Smart Mater. Med.*, 2022, **3**, 230–242.

56 K. Yang, J. Li, M. Lamy de la Chapelle, G. Huang, Y. Wang, J. Zhang, D. Xu, J. Yao, X. Yang and W. Fu, *Biosens. Bioelectron.*, 2021, **175**, 112874.

57 S. Kaushal, A. K. Pinnaka, S. Soni and N. K. Singhal, *Sens. Actuators, B*, 2021, **329**, 129141.

58 X. Gan, F. Qiu, B. Jiang, R. Yuan and Y. Xiang, *Sens. Actuators, B*, 2021, **332**, 129483.

59 S. Bhattacharjee, P. Subha, M. Paul Das, M.-R. Ganesh, Y.-B. Shim, B. Neppolian and J. Das, *Appl. Surf. Sci.*, 2021, **541**, 148517.

60 F. Xu, H. Tang, J. Yu and J. Ge, *Talanta*, 2021, **224**, 121838.

61 W. Qi, L. Zheng, S. Wang, F. Huang, Y. Liu, H. Jiang and J. Lin, *Biosens. Bioelectron.*, 2021, **178**, 113020.

62 M. Hu, L. Zhu, Z. Li, C. Guo, M. Wang, C. Wang and M. Du, *Appl. Surf. Sci.*, 2021, **542**, 148586.

63 M. Nazari, A. S. Saljooghi, M. Ramezani, M. Alibolandi and M. Mirzaei, *J. Mater. Chem. B*, 2021, **10**, 8824–8851.

64 X. Ma, M. Lepoitevin and C. Serre, *Mater. Chem. Front.*, 2021, **5**, 5573–5594.

65 N. Huang, P. Wang and D. Jiang, *Nat. Rev. Mater.*, 2016, **1**, 16068.

66 S. Xu and Q. Zhang, *Mater. Today Energy*, 2021, **20**, 100635.

67 S. Wan, J. Guo, J. Kim, H. Ihee and D. Jiang, *Angew. Chem., Int. Ed.*, 2008, **47**, 8826–8830.

68 S. Dalapati, E. Jin, M. Addicoat, T. Heine and D. Jiang, *J. Am. Chem. Soc.*, 2016, **138**, 5797–5800.

69 R. Gomes and A. Bhaumik, *RSC Adv.*, 2016, **6**, 28047–28054.

70 H. L. Qian, C. Dai, C. X. Yang and X. P. Yan, *ACS Appl. Mater. Interfaces*, 2017, **9**, 24999–25005.

71 S. Wang, L. Ma, Q. Wang, P. Shao, D. Ma, S. Yuan, P. Lei, P. Li, X. Feng and B. Wang, *J. Mater. Chem. C*, 2018, **6**, 5369–5374.

72 J. Zeng, X. Wang, B. Xie, M. Li and X. Zhang, *Angew. Chem., Int. Ed.*, 2020, **59**, 10087–10094.

73 T. Skorjanc, D. Shetty and M. Valant, *ACS Sens.*, 2021, **6**, 1461–1481.

74 N. Huang, X. Ding, J. Kim, H. Ihee and D. Jiang, *Angew. Chem., Int. Ed.*, 2015, **54**, 8704–8707.

75 H. Q. Yin, F. Yin and X. B. Yin, *Chem. Sci.*, 2019, **10**, 11103–11109.

76 J. Dong, X. Li, S. B. Peh, Y. D. Yuan, Y. Wang, D. Ji, S. Peng, G. Liu, S. Ying, D. Yuan, J. Jiang, S. Ramakrishna and D. Zhao, *Chem. Mater.*, 2019, **31**, 146–160.

77 J. Jin, H. Jiang, Q. Yang, L. Tang, Y. Tao, Y. Li, R. Chen, C. Zheng, Q. Fan, K. Y. Zhang, Q. Zhao and W. Huang, *Nat. Commun.*, 2020, **11**.

78 S. Kang, H. Ahn, C. Park, W. H. Yun, J. G. Jeong, Y. J. Lee and D. W. Kim, *Adv. Sci.*, 2023, **10**.

79 G. Das, F. Benyettou, S. K. Sharama, T. Prakasam, F. Gándara, N. I. Saleh, R. Pasricha, R. Jagannathan, M. A. Olson and A. Trabolsi, *Chem. Sci.*, 2018, **9**, 8382–8387.

80 J. You, F. Yuan, S. Cheng, Q. Kong, Y. Jiang, X. Luo, Y. Xian and C. Zhang, *Chem. Mater.*, 2022, **34**, 7078–7089.

81 F. Yuan, Y. Kong, J. You, C. Zhang and Y. Xian, *ACS Appl. Mater. Interfaces*, 2021, **13**, 51351–51361.

82 L. Liao, Z. Zhang, X. Guan, H. Li, Y. Liu, M. Zhang and Q. Fang, *Chin. J. Chem.*, 2022, **40**, 2081–2088.

83 D. Zhen, S. Zhang, A. Yang, L. Li, Q. Cai, C. A. Grimes and Y. Liu, *Int. J. Biol. Macromol.*, 2023, 129104.

84 P. Wang, F. Zhou, C. Zhang, S. Y. Yin, L. Teng, L. Chen and X. B. Zhang, *Chem. Sci.*, 2018, **9**, 8402–8408.

85 P. Sun, J. Hai, S. Sun, S. Lu, S. Liu, H. Liu, F. Chen and B. Wang, *Nanoscale*, 2020, **12**, 825–831.

86 P. Gao, K. Tang, R. Lou, X. Liu, R. Wei, N. Li and B. Tang, *Anal. Chem.*, 2021, **93**, 12096–12102.

87 P. Gao, R. Wei, Y. Chen, X. Liu, J. Zhang, W. Pan, N. Li and B. Tang, *Anal. Chem.*, 2021, **93**, 13734–13741.

88 T. Skorjanc, D. Shetty, S. Kumar, D. Makuc, G. Mali, J. Volavsek, M. B. Marusic and M. Valant, *Chem. Commun.*, 2023, **59**, 5753–5756.

89 Y. Pan, X. Luan, F. Zeng, Q. Xu, Z. Li, Y. Gao and Y. Song, *Biosens. Bioelectron.*, 2022, **209**, 114239.

90 P. Gao, J. Yin, M. Wang, R. Wei, W. Pan, N. Li and B. Tang, *Anal. Chem.*, 2022, **94**(38), 13293–13299.

91 B. Wang, X. Liu, P. Gong, X. Ge, Z. Liu and J. You, *Chem. Commun.*, 2020, **56**, 519–522.

92 P. Gao, X. Shen, X. Liu, Y. Chen, W. Pan, N. Li and B. Tang, *Anal. Chem.*, 2021, **93**, 11751–11757.

93 G. Kaur, D. Kumar, S. Sundarrajan, S. Ramakrishna and P. Kumar, *Polymers*, 2022, **15**(1), 139.

